Journal of Radiation and Nuclear Applications
An International Journal

http://dx.doi.org/10.18576/jrna/050307

Assessment of the Elemental Concentration of Potassium, Uranium and Thorium with their Associated Radiogenic Heat Production in Granite Rocks of Southwestern Nigeria

S. T. Gbenu[1], S. F. Olukotun[2], O. F. Oladejo[3], C. A. Onumejor[2], F. O. Balogun[4], F. I. Ibitoye[1], M. K. Fasasi[1]*

[1] Centre for Energy Research and Development (CERD), Obafemi Awolowo University, Ile-Ife, Nigeria.
[2] Department of Physics and Engineering Physics, Obafemi Awolowo University, Ile-Ife, Nigeria.
[3] Department of Department of Physics, Osun State University, Oshogbo, Osun, Nigeria.
[4] Department of Earth Sciences, University of Oregon, Eugene, Oregon 97403, USA.

Received: 18 Jun.2020, Revised: 21 Jul.2020, Accepted: 13 Aug.2020.

Published online: 1 Sep. 2020.

Abstract: Radiogenic heat production (RHP) was evaluated from the elemental concentrations of Potassium (K), Thorium (Th) and Uranium (U) in granite rocks of southwest Nigeria using gamma ray spectrometry. The mean K, Th and U values of 2.71%, 30.57 ppm and 3.02 ppm, respectively were obtained for the entire study area. The abundance ratios (K/Th, K/U, Th/U) were calculated in order to study the enrichment/depletion processes in the granite rocks of the sub region. A mean value of 3.14μWm^{-3}obtained for the RHP is comparable to the world average value of 3μWm^{-3} for granite rocks and the abundance ratios indicates a depletion of uranium from its ore. All variables were subjected to multivariate statistical analysis to determine the various relationships that exist among them. Principal component analysis (PCA) yields a three component representation of the acquired data in which 91.2% of the total variance was explained.

Keywords: Granite; Elemental concentration; Radiogenic heat production; Gamma ray spectrometry; Southwest Nigeria

1 Introduction

Potassium, Thorium and Uranium are long lived radioactive elements in the earth crust. The specific levels of terrestrial environmental radiation are related to the geological composition of each lithologically separated area, and to the content in thorium (Th), uranium (U) and potassium (K) of the rock from which the soils originate in each area [1 – 3]. The concentration of radionuclides like uranium, thorium and potassium are high in granite rocks. The uranium and thorium integrated during the crystallization of magma and residual solutions because their large ionic radii prevent their crystallization out of the early silicates [4].

The average concentration of uranium in the earth crust has been reported to be in the range of 2–3 ppm, while thorium exists in the range of 8–12 ppm [5]. Potassium is widely distributed in nature, with concentrations varying from about 0.1% for limestone, through 1% for sandstones to as much as 3.5% for some granite rocks [6]. The concentrations of major and trace elements in Environmental samples had been studied by several authors [7 – 11].

However, there is a need to examine the elemental concentration of these radionuclides in the bedrocks from which soil emanates, as well as, their respective elemental abundance ratio (Th/U, K/U, and K/Th ratios). This analysis will also allow us to study the enrichment/depletion processes as a result of the complex metamorphic history, alteration and/or weathering that affected the rocks over the course of time [12].

Works have been carried out on the estimation of radiogenic heat production from the elemental concentrations of radio-elements measured in the laboratory [13] and directly from gamma-ray data [14]. Similarly, airborne gamma ray data has been used to estimate radiogenic heat production [13].
Assessment of the radiogenic heat production can be used for the explanation of temperature variations with depth and interpretation of existing heat flow variations. Also it can be used in selecting suitable new sites for making heat flow

*Corresponding author e-mail: olukotunsf@oauife.edu.ng

and heat production measurements. This work will provide a new insight to the geothermal properties of the quarries in southwest Nigeria.

2 Experimental Sections

2.1 Sample Collection and Preparation

A total of fifty (50) samples were collected from ten (10) different quarry sites (five samples from each site) spread across five states (Ogun, Oyo, Osun, Ondo and Ekiti) of Southwest Nigeria. The coordinates of each sample location were taken and recorded [15]. Each sample was crushed, dried, sieved and hermetically sealed in cylindrical polyvinylchloride containers for 28 days in order to attain secular equilibrium between the parent and the daughter nuclides present.

2.2 Gamma Ray Spectroscopic Technique

The activity concentration of natural radioactivity in the samples were determined using a 7.62 cm x 7.62 cm NaI (Tl) detector employed with adequate lead shielding which reduced the background by a factor of about 95%. The activities of various radionuclides were determined in Bq kg^{-1} using the count spectra obtained from each of the samples. The gamma ray photo peaks corresponding to energy of 1120.3 keV (^{214}Bi), 911.21 keV (^{228}Ac) and 1460.82 keV (^{40}K) were considered to determine the activity of ^{238}U, ^{232}Th and ^{40}K [15 – 17]. The Minimum Detectable Activity was calculated as 11.40, 12.85 and 6.77 Bq kg^{-1} for ^{232}Th, ^{238}U and ^{40}K, respectively for a counting time of 25,200 seconds.

2.3 Determination of Elemental Concentration

The assessment of the potassium elemental concentration in rocks, soil and water is expressed in percentage potassium (%K) and part per million (ppm) for uranium and thorium. In using gamma ray spectrometry, the 1460 keV gamma ray energy emitted by ^{40}K was used for the assessment of potassium. The estimation of ^{40}K is direct because it occurs in nature as a fixed ratio to other isotopes of potassium. However, the estimation of uranium and thorium were obtained indirectly through the energy lines of their daughter products, 1120.3 keV (^{214}Bi) and 911.21keV (^{228}Ac), respectively (IAEA, 2003). The IAEA provides a conversion factor of 1% K in rock to be equivalent to 313 Bq kg^{-1}, 1.0 ppm U in rock to be equivalent to 12.35 Bq kg^{-1} and 1.0 ppm Th in rock equals 4.06 Bq kg^{-1} [5]. These values agree with Equation 1 [18].

$$C_E = \frac{M_E \Omega}{\lambda_E N_A f_A} A_E, \quad (1)$$

where C_E is the fraction of element E in the sample, M_E is the atomic mass ($kgmol^{-1}$), λ_E is the decay constant (s^{-1}), f_A, is the fractional atomic abundance in nature and A_E is the measured activity concentration ($Bqkg^{-1}$), of the corresponding radionuclide considered (^{232}Th, ^{238}U, or ^{40}K), N_A is the Avogadro's number (6.023×10^{23} atoms mol^{-1}), and Ω is a constant with a value of 1,000,000 for ^{232}Th and ^{238}U, and 100 for ^{40}K. The elemental concentrations are thus reported in units of μg g^{-1}or ppm for thorium and uranium, and as a percentage (%) for potassium.

2.4 Calculation of Radiogenic Heat Production

Estimates of ^{40}K, ^{238}U and ^{232}Th concentrations from gamma ray spectrometry can be used to evaluate the heat generated by rocks. Disintegration of the natural radionuclides in the earth is accompanied by the release of thermal energy, and most of this is produced by the decay of ^{40}K, ^{238}U and ^{232}Th. The heat production (HP) of rocks is related to the concentration of the radioelements C_K (% K), C_U (ppm U), C_{Th} (ppm Th), and density of rock ρ (kg m^{-3}) by Equation 2 [5, 19].

$$HP = \rho(3.48C_k + 9.52C_u + 2.56C_{Th}) * 10^{-5} \quad (\mu Wm^{-3}) \quad (2)$$

Where C_K, C_U, and C_{Th} are the elemental concentrations of ^{40}K, ^{238}U and ^{232}Th, respectively in % for ^{40}K and ppm for ^{238}U and ^{232}Th. The density of the granite samples is between 2650 and 2750 kgm^{-3}, however, an average value of 2700 kgm^{-3} was used.

3 Results and Discussion

3.1 Elemental Concentration

The elemental concentration of each of the samples is presented in columns 2 to 4 of Table 1. The concentration of ^{232}Th is generally higher with an average value of 30.57 ppm and a maximum value 138.22 ppm for the sample code named, OGA1 while ^{238}U and ^{40}K have a range of ND to 8.96 ppm and 0.43 to 5.78 %, respectively. The average values of 2.71% for ^{40}K, 30.57ppm for ^{232}Th and 3.02 ppm for ^{238}U, obtained for the entire sampled quarry are higher than the world average concentration of 1.3 % for ^{40}K, 7.4 ppm for ^{232}Th and 2.8 ppm for ^{238}U in granite rocks. These average values were obtained by converting the corresponding worldwide average activity concentrations of 30, 35, and 400 $Bqkg^{-1}$ [20] for ^{232}Th, ^{238}U and ^{40}K radionuclides, into their respective elemental concentrations using the Equation 1

3.2 Elemental Abundance Ratio

The elemental abundance ratios of K/U, K/Th, and Th/U are given in column 5 to 7 of Table 1. These ratios are an indication of the relative depletion or enrichment of radioisotopes. The average value of 1.08 and a maximum

Value of 9.89 for the K/U ratio indicate that the values of U are lower than that of K in the rock samples. This is expected as granite rocks have a higher concentration of potassium oxide than any oxides of uranium. In the same vein, the average value of 0.16 obtained for the K/Th ratio indicates a much higher value of Th than K. However, from the table, the Th/U value are generally high with a range of 0.73 – 51.21, and an average value of 10.78. A Th/U ratio higher than 1 is significant [21]. Although U and Th are geochemically similar, the average Th/U ratio obtained is far from 3.0, 3.5 and 4.25 that have been reported in literatures [12, 22, 23] for a normal continental crust. The high Th/U ratios describe an initially fertile granite rock, but leached out its U content leaving Th behind.

3.3 Radiogenic Heat Production

The calculated radiogenic heat production (RHP) is governed by the amount of uranium, thorium, and potassium measured in each sample and as a result varied from one sample to another. The results, as presented in column 8 of Table 1 show a similar trend within each quarry location, with the values though different have a narrow range. This irregularity is due partly to the probabilistic nature of radioactive decay from which the concentrations were calculated and to the dissimilarity in the geochemical activities of ^{40}K, ^{238}U and ^{232}Th during the transformation process. On the other hand, the heat generated varies greatly across the quarries of the southwestern Nigeria. This is evident in the total range of 0.57 – 10.69 μWm^{-3} and a mean value of 3.14 μWm^{-3}. This result agrees with the literature radiogenic heat production value of 3$\mu Wm^{-3}$for granite rocks [24]. It is of note that the mean value of each quarry location ranged from 1.34μWm^{-3} to 6.28 μWm^{-3}. This demonstrates the fact that heat production in granite shows a lot of variability both between and within intrusions [24 – 25].

Table 1: Elemental concentration, Abundance ratio and Radiation heat Generated.

	^{40}K (%)	^{232}Th (ppm)	^{238}U (ppm)	K/U	K/Th	Th/U	RHP(μWm^{-3})
GCA1	1.14	138.22	3.99	0.29	0.01	34.67	10.69
GCA2	0.63	27.44	3.60	0.17	0.02	7.61	2.88
GCA3	0.39	22.59	3.56	0.11	0.02	6.34	2.51
GCA4	2.03	40.47	0.79	2.57	0.05	51.21	3.19
GCA5	3.25	78.11	4.03	0.81	0.04	19.37	6.74
Mean	**1.49**	**61.36**	**3.19**	**0.47**	**0.02**	**19.21**	**5.20**
GCB1	2.16	12.94	3.07	0.70	0.17	4.21	1.89
GCB2	2.26	31.90	2.95	0.76	0.07	10.80	3.18
GCB3	1.85	15.99	3.13	0.59	0.12	5.11	2.08
GCB4	3.04	35.23	3.25	0.93	0.09	10.84	3.56
GCB5	2.35	11.41	2.99	0.78	0.21	3.82	1.78
Mean	**2.33**	**21.49**	**3.08**	**0.76**	**0.11**	**6.98**	**2.50**
GCC1	1.21	46.41	2.63	0.46	0.03	17.63	4.00
GCC2	0.53	18.18	2.61	0.20	0.03	6.95	1.98
GCC3	1.98	39.54	2.73	0.72	0.05	14.47	3.62
GCC4	0.00	29.40	2.40	0.00	0.00	12.25	2.65
GCC5	2.85	16.06	1.83	1.56	0.18	8.77	1.85
Mean	**1.31**	**29.92**	**2.44**	**0.54**	**0.04**	**12.25**	**2.82**
GCD1	5.36	53.37	4.98	1.08	0.10	10.72	5.47
GCD2	5.68	72.74	4.93	1.15	0.08	14.77	6.83
GCD3	8.96	62.37	4.66	1.92	0.14	13.38	6.35
GCD4	7.22	76.49	4.56	1.58	0.09	16.77	7.14
GCD5	6.23	57.06	4.24	1.47	0.11	13.44	5.62
Mean	**6.69**	**64.41**	**4.67**	**1.43**	**0.10**	**13.78**	**6.28**
GCE1	0.71	29.15	1.85	0.38	0.02	15.73	2.56
GCE2	2.42	27.78	3.54	0.68	0.09	7.85	3.06
GCE3	2.51	17.05	1.23	2.05	0.15	13.89	1.73
GCE4	0.45	10.52	2.57	0.17	0.04	4.10	1.43
GCE5	6.88	4.55	2.71	2.54	1.51	1.68	1.66
Mean	**2.59**	**17.81**	**2.38**	**1.09**	**0.15**	**7.49**	**2.09**
GCF1	0.91	35.00	2.29	0.40	0.03	15.26	3.09
GCF2	0.69	44.91	1.96	0.35	0.02	22.86	3.67
GCF3	3.56	29.53	1.24	2.87	0.12	23.79	2.70
GCF4	2.80	38.05	2.35	1.19	0.07	16.23	3.50
GCF5	3.95	23.26	2.49	1.59	0.17	9.35	2.62
Mean	**2.38**	**34.15**	**2.07**	**1.15**	**0.07**	**16.53**	**3.12**
GCG1	5.18	29.00	3.37	1.54	0.18	8.61	3.36
GCG2	4.26	14.48	2.70	1.58	0.29	5.37	2.10
GCG3	0.25	10.26	2.09	0.12	0.02	4.91	1.27
GCG4	4.29	2.72	0.43	9.89	1.58	6.28	0.70
GCG5	2.55	26.59	2.55	1.00	0.10	10.42	2.73
Mean	**3.31**	**16.61**	**2.23**	**1.48**	**0.20**	**7.45**	**2.03**
GCH1	0.22	1.31	1.79	0.12	0.17	0.73	0.57
GCH2	0.26	10.13	2.42	0.11	0.03	4.19	1.35
GCH3	0.22	13.94	2.07	0.11	0.02	6.74	1.52
GCH4	0.41	14.31	2.11	0.19	0.03	6.79	1.57
GCH5	0.95	14.78	2.30	0.41	0.06	6.42	1.70
Mean	**0.41**	**10.89**	**2.14**	**0.19**	**0.04**	**5.10**	**1.34**
GCI1	3.96	18.26	3.04	1.30	0.22	6.01	2.41
GCI2	4.51	41.10	3.75	1.20	0.11	10.95	4.23
GCI3	7.11	29.40	3.50	2.03	0.24	8.41	3.60
GCI4	4.78	43.56	3.57	1.34	0.11	12.19	4.38
GCI5	3.87	20.31	3.45	1.12	0.19	5.88	2.66
Mean	**4.85**	**30.52**	**3.46**	**1.40**	**0.16**	**8.82**	**3.46**
GCJ1	0.80	17.59	5.78	0.14	0.05	3.04	2.78

GCJ2	1.43	5.10	4.32	0.33	0.28	1.18	1.60
GCJ3	1.44	15.33	4.93	0.29	0.09	3.11	2.46
GCJ4	3.13	33.48	3.98	0.79	0.09	8.41	3.63
GCJ5	1.98	20.93	3.88	0.51	0.09	5.39	2.63
Mean	**1.76**	**18.49**	**4.58**	**0.38**	**0.10**	**4.04**	**2.62**

3.4 Multivariate Statistical Analysis

Multivariate analysis involves observation and analysis of more than one statistical outcome variables at a time. It shows how the variables are related to one another, thus enhances data interpretation. The statistical analysis considered in this work are, Principal Component analysis, Pearson Correlation Coefficients and Hierarchical Cluster Analysis, load plot.

3.5 Descriptive statistic

Descriptive statistics show the raw scores, organized and summarized in a form that enhances readability. It provides a single descriptive overview of the entire data set [26]. The list of statistical variables is presented in Table 2. It can be seen from the table that, of the 50 samples studied, ^{232}Th has the highest value of 138 ppm, while the minimum concentration was observed in ^{40}K (BDL). Considering the mean values K/U, K/Th, Th/U and RHP it can easily be observed that they are close to the standard deviation in spite of the differences in values from each location.

Table 2: Descriptive Statistics

Variables	N	Mean	SD	Sum	Min	Max
^{40}K	50	2.71	2.19	135.60	0.00	8.96
^{232}Th	50	30.57	24.15	1528.28	1.31	138.22
^{238}U	50	3.02	1.13	151.20	0.43	5.78
K/U	50	1.08	1.46	54.23	0.00	9.89
K/Th	50	0.16	0.30	7.76	0.00	1.58
Th/U	50	10.78	8.69	538.91	0.73	51.21
RHP	50	3.14	1.88	157.24	0.57	10.69

3.6 Principal Component Analysis

Principal component analysis (PCA) is a very useful tool for discovering previously unsuspected relationships as well as reducing and interpreting large multivariate data sets with underlying linear structures. Table 3 presents the list of variables and their corresponding principal component coefficients. The principal component analysis yields a three component representation of the acquired data, in which 91.2% of the total variance was explained. This value is a good result because a value that explained 75% or more of the total variance is good [27].

The first component explained 41.63% of the total variance and it is heavily loaded for ^{232}Th and RHP associated with all samples. Principal component 2 has a strong positive loading for K and K/Th and account for 29.99% of the total variance while component 3 explained 19.54% of the total variance with a positive loading for ^{238}U.

Table 3: Principal component.

Variables	Principal Components		
	1	**2**	**3**
^{40}K	0.20003	**0.51049**	0.33815
^{232}Th	**0.55889**	0.09468	-0.13146
^{238}U	0.33595	-0.08163	**0.65306**
K/U	-0.1463	0.6238	-0.15558
K/Th	-0.26283	**0.55419**	0.10037
Th/U	0.34783	0.10675	-0.63809
RHP	**0.56859**	0.12696	0.02111
Variance Explained %	**41.63%**	**29.99%**	**19.54%**

3.7 Pearson Correlation Analysis

All the evaluated variables were subjected to Pearson correlation analysis in order to determine the mutual relations and the degree of association that exist between pairs of variables. The correlation coefficient matrix of all the radiological variables examined is presented in Table 4. The strength of the correlation is defined for the absolute value of the Pearson coefficient as, 0.00 – 0.19 (very weak), 0.20 – 0.39 (weak), 0.40 – 0.59 (moderate), 0.60 – 0.79 (strong) and 0.80 – 1.0 (very strong). It can be seen from the table that a strong positive correlation exists among ^{232}Th and Th/U and between ^{232}Th and ^{238}U because thorium and uranium exist together in nature [28]. The thorium is a major contributor in the RHP values [29, 30]. Similarly, a positive moderately strong correlation was observed between ^{40}K and K/U and between ^{40}K and K/Th. On the other hand, weak negative correlations were observed between, ^{232}Th and K/U and between ^{232}Th and K/Th. This is expected as K does not belong to the same series with ^{232}Th and ^{238}U. ^{238}U has a weak negative correlation with K/U, K/Th and Th/U but has a strong positive correlation with RHP.

3.8 Loading Plot

The Loading plot shows the relationships between variables in the space of the first two principal components. The loading plot (Figure 1) shows the relationship of the variables in relation to principal components 1 and 2. We observed that ^{40}K, K/U and K/Th have a positive heavy loading for principal component 2 while, Th/U, ^{232}Th, ^{238}U and RHP have similar positive heavy loading for principal component 1.

3.9 Hierarchical Custer Analysis

Hierarchical Cluster Analysis is one of the methods of carrying out a cluster analysis. Cluster analysis is a multivariate method in which items/objects are classified

on the basis of a set of measured variables into a number of different groups such that items/objects in the same group are similar.

A visual display of the order in which parameters or variables with related properties combine to form clusters is done with the dendrogram. The most similar objects are first grouped and merged according to their similarities. Similarity is a measure of the distance between clusters in relation to the largest distance between any two variables. The dendrogram is the most important result of cluster analysis. It lists all samples and indicates at what level of similarity any two clusters were joined. The position of the line on the scale indicates the distance at which clusters were joined. The top of the unit for each stage represents the new cluster by the merging of two clusters. Its height corresponds to the distance between two merged clusters.

Presented in Figure 2, is the dendrogram; a result of cluster analysis, showing all variables and indicates at what level of similarity any two clusters were joined. All the 7 variables are grouped into fours statistically significant clusters. Cluster-I consists of ^{40}K, cluster-II consists of K/U and K/Th, cluster-III consists of ^{232}Th, Heat Generated and Th/U, and finally, cluster-IV consists of ^{238}U. All the clusters are formed on the basis of existing similarities.

Table 4: Correlation coefficient matrix.

	^{40}K	^{232}Th	^{238}U	K/U	K/Th	Th/U	RHP
^{40}K	1						
^{232}Th	0.30548	1					
^{238}U	0.34267	0.40061	1				
K/U	0.46296	-0.0841	-0.35069	1			
K/Th	0.38036	-0.29071	-0.23586	**0.77008**	1		
Th/U	0.05421	**0.65486**	-0.21072	0.11194	-0.23387	1	
RHP	0.43245	**0.98075**	**0.54632**	-0.07804	-0.25234	0.55343	1

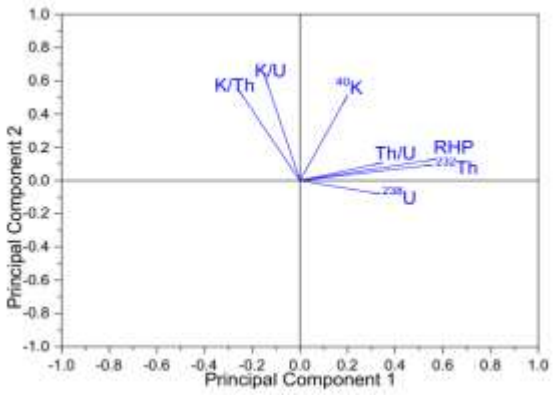

Fig.1: Loading Plot.

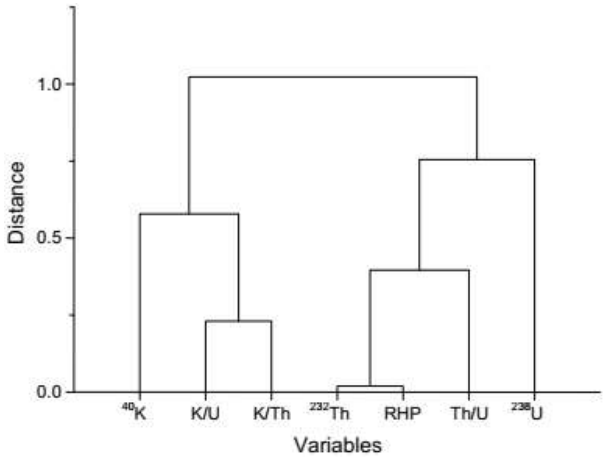

Fig.2: Dendrogram showing clusters of the concentrations and radioactive heat production.

3 Conclusions

The elemental concentration of potassium, thorium and uranium in the granite rocks of southwest Nigeria were estimated. The concentrations in the studied area were found to be higher than the world average value. Similarly, the average elemental abundance ratio was found to be higher than published values for normal continental crust. However, the radiogenic heat production from granite rocks in the sub-region was estimated and the results agree with the literature value of 3μWm^{-3} for granite rocks. Multivariate analysis has proven to be an appropriate means of interpreting data of the types considered in this work.

Acknowledgement: We acknowledge the Centre for Energy Research and Development (CERD), Obafemi Awolowo University, Ile-Ife, Osun State, Nigeria for allowing us to use their Gamma Spec laboratory for the analysis

References

[1] E. O. Ojo, H. O. Shittu, A. A. Adelowo, B. N. Ossai, C. B. Emefiene (2015). The model of radiogenic heat production in the Federal Capital Territory (FCT) Abuja, Nigeria. International Journal of Modern Physics and Applications., **1 (5)**, 200 – 204(2015).

[2] AA Shaltout, SI Ahmed, SD Abayazeed, A El-Taher, OH Abd-Elkader Quantitative elemental analysis and natural radioactivity levels of mud and salt collected from the Dead Sea, Jordan. Microchemical Journal., **133**, 352-357(2016)

[3] A. El-Taher and H. Madkour Environmental studies and Radio-Ecological Impacts of Anthropogenic areas: Shallow Marine Sediments Red Sea, Egypt. Journal of Isotopes in Environment and Health Studies., **50**, 120 -133(2014).

[4] Shiva N. G., Prasad N., Nagaiah G. V., Ashok, T., and Karunakara. (2008). Concentrations of Ra-226, Th 232 and K-40 in the soil of Bangalore Region, India.Health Phys., **94 (3)**, 246-271(2008).

[5] IAEA (2003). Guidelines for radioelement mapping using gamma ray spectrometry data. IAEA-TECDOC 1363. International Atomic Energy Agency, Vienna, Austria.

[6] MB Challan and A El-Taher Analytical approach for radioactivity correlation of disc sources with HPGe detector efficiency. Applied Radiation and Isotopes., **85**, 23-27(2014).

[7] Dragovic S. L., Onjia A., & Bacic G. (2006). Distribution of primordial radionuclides in surface soils from Serbia and Montenegro. Radiation Measurement., **41**, 611–616(2006).

[8] Fagbote E. O., & Olanipekun E. O. (2010). Evaluation of the status of heavy metal pollution of soil and plant (Chromolaena odoranta) of Agbabu bitumen deposit area, Nigeria. American-Eurosian J Sci Res., **5(4)**, 241–248(2010).

[9] Zheng L. G., Liu G. J., Kang Y., & Yang R. K. (2010). Some potential hazardous trace elements contamination and their ecological risk in sediments of western Chaohu Lake, China. Environ Monit Assess., **166**, 379–386(2010).

[10] Ali S. M., & Malik R. N. (2011). Spatial distribution of metals in top soils of Islamabad City, Pakistan. Environ Monit Assess., **172**, 1–16(2011).

[11] Omoniyi I. M., Oludare S. M., Oluwaseyi O. (2013). Determination of radionuclides and elemental composition of clay soils by gamma- and X-ray spectrometry. 2,. SpringerPlus., **74**, (2013).

[12] Chiozzi P., Pasquale, V., & Verdoya M. (2002). Naturally occurring radioactivity at the Alps Apennines transition. . Radiation Measurements , **35**,147–154(2002)..

[13] Richardson K. A., Killeen P. G. (1980). Regional radiogenic heat production mapping by airborne gamma-ray spectrometry. Current Research, Part B, Geological Survey of Canada **(Paper 80-1B)**, 227-232(1980)..

[14] Bücker C., & Rybach L. (1996). A simple method to determine heat production from gamma-ray logs, Marine and Petroleum Geology., **13**, 373-375(1996)..

[15] Gbenu S. T., Oladejo O. F., Alayande O., Olukotun S. F., Fasasi M. K., & Balogun F. A. (2016a). Assessment of Radiological Hazard of Quarry products from Southwest Nigeria. Journal of Radiation Research and Applied Sciences, **9(1)**, 20-25(2016a)..

.[16] Kehinde Aladeniyi, Christopher Olowookere & Bosede Blessing Oladele (2019). Measurement of natural radioactivity and radiological hazard evaluation in the soil samples collected from Owo, Ondo State, Nigeria. Journal of Radiation Research and Applied Sciences., 12:1, 200-209(2019).

[17] Makinde O. W., Oluyemi E. A., Adesiyan A. T.,Ogundele K. T., Gbenu S. T., Fadodun O. G. (2020).Radiation dose level of natural radionuclide in plantain leaves around a gold mining environment in South West Nigeria. J. Rad. Nucl. Appl. **5(1)**, 47-53(2020).

[18] Tzortis M., & Tsertos H. (2004). Determination of thorium, uranium and potassium elemental concentrations in surface soils in Cyprus. Environmental Rdioactivity., **77 (3)**, 325-328(2004).

[19] Rybach L. (1976). Radioactive heat production in rocks and its relation to other petrophysical parameters. Pure & Appl. Geophysics., **114**, 309-318(1976).

[20] UNSCEAR. (2000). Effects and Risks of Ionizing Radiation. Report to the General Assembly with Annex B. New York: United Nations Scientific committee on Effects of Atomic Radiation.

[21] Rogers J., and Adams J. (1969). Thorium. In K. Wedepohl, Handbook of Geochemistry, Part II/I (p. 39). Berlin : Springer Verlag.

[22] A El-Taher, A. Nossair, A.H. Azzam, K.-L. Kratz and A.S. Abdel-Halim Determination of Traces of Uranium and Thorium in Some Egyptian Environmental Matrices by Instrumental Neutron Activation Analysis. Journal of Environmental protection engineering., **29(1-2)**, 19-30 (2004).

[23] Ravisankar R., Chandrasekaran A., Senthilkumar G., Thillaivelavan K., Dhinakaran B., Vijayagopal, P., et al. (2014). Spatial distribution and lifetime cancer risk due to gamma radioactivity in Yelagiri Hills, Tamilnadu, India.Egyptian Journal of Basic and Applied Sciences., 1, 38 – 48(2014).

[24] A. El-Taher and WR Alharbi Elemental analysis of hematite by instrumental neutron activation analysis. Life Science Journal., **9(4)**, 2011.

[25] Sun Zhanxue; Wang Andong; Liu Jinhui; Hu Baoqun; Chen Gongxin. (April 2015). Radiogenic Heat Production of Granites and Potential for Hot Dry Rock Geothermal Resource in Guangdong Province, Southern China. Proceedings World Geothermal Congress (pp. 19-25). Melbourne, Australia: World Geothermal Congress.

[26] Gbenu S. T., Oladejo O. F., Olukotun S. F., Makinde O. W., Fasasi M. K., & Balogun F. A. (2016b). Assessment of radioactivity and radiological hazards in commercial ceramic tiles used in Ife-Centra, local government area of Osun State, Nigeria. Egyptian Journal of BasiC and Applied Science .

[27] Zhang H., Lu Y., Dawson R. W., Shi Y., & Wang T. (2005). Classification and Ordination of DDT and HCH in soil samples from the Guanting Reservoir, China. Chemosphere., **60**, 762–769(2005).

[28] Tanaskovi I., Golobocanin D., & Milijevic N. (2012). Multivariate statistical analysis of hydrochemical and radiological data of Serbian spa waters. J. Geochem. Explor., **112**, 226-234(2012).

[29] Thompson P. H., Judge A. S., Charbonneau B. W., Carson J. M., & Thomas, M. D. (1996). Thermal regimes and diamond stability in the Archean Slave Province, Northwestern Canadian Shield, District of Mackenzie, Northwest Territories;. (Current Research, 96-1), 135-146(1996).

[30] Fernández M., Marzan I., Correia A., & Ramalho E. (1998). Heat flow, heat production, and lithosphere thermal regime in the Iberian Peninsula,. Tectonophysics., **291**, 29-53(1998).